Journal of Materials Chemistry B

Accepted Manuscript

ROYAL SOCIETY OF CHEMISTRY

www.rsc.org/materialsB

Journal of Materials Chemistry B RSCPublishing

ARTICLE

A Combined "RAFT" and "Graft From" Polymerization Strategy for Surface Modification of Mesoporous Silica Nanoparticles: Towards Enhanced Tumor Accumulation and Cancer Therapy Efficacy

Cite this: DOI: 10.1039/x0xx00000x

Received ooth January 2012,
Accepted ooth January 2012

DOI: 10.1039/x0xx00000x

www.rsc.org/

Ming Ma,[a] Shuguang Zheng,[b] Hangrong Chen,[*,a] Minghua Yao,[b] Kun Zhang,[a] Xiaoqing Jia,[a] Juan Mou,[a] Huixiong Xu,[b] Rong Wu,[b] and Jianlin Shi [*, a]

A novel modification route integrating the copolymer of positive charged quaternary amines and polyethylene glycol (PEG) units using a combination of Reversible Addition Fragmentation chain Transfer polymerization (RAFT) and "Graft From" strategy, has been proposed, for the first time, to decorate the surface of mesoporous silica nanoparticles (MSNs), towards the smallest hydrodynamic size of particles in physiological solution. It is demonstrated that such efficient copolymer surface modification strategy, resulting in PEG coating with high positive zeta potential, can achieve nearly 2 folds of enhanced permeability and retention (EPR) effect, and longer blood half-life compared to coating with PEG only. Besides, the *in vivo* results demonstrated that this surface modification strategy could lead to a higher efficacy of doxorubicin drug delivery and greater suppressed side effect compared to the free drug. Based on this novel strategy of combined "RAFT" and "Graft From" polymerization, it is hopeful that this efficient modification towards tumor specific targeting of MSNs can be widely used in the further nanomedicine researches.

1. Introduction

Mesoporous silica nanoparticles (MSNs) have received extensive attentions in the past decade in the field of cancer treatments due to their potential applications in drug/gene delivery and cell imaging. [1,2] Compared to conventional polymeric nanoparticles, such as poly(lactic-co-glycolic acid (PLGA), phospholipid and protein capsules, MSNs shows a number of distinctive merits including high mechanical strength, biocompatibility and resistance to microbial attack, etc. More importantly, the high surface area and large amount of silanols in the internal surface of MSNs enable the preferential absorption of free drug molecules by electrostatic attraction, hydrogen-bonding or van der Waals forces, generally showing the much higher drug payload than organic delivery carriers. However, as a new generation drug delivery system (DDS), various challenges need to be overcome for the future successful translation from bench to bedsides of MSNs, especially, homogeneous size-distribution, well dispersity in physiological solution, high passive targeting efficiency, and long blood half-life period, etc.

Modern trends in MSNs DDS design and fabrication are rationally focused on the reduction of actual size of MSNs in physiological solution for enhanced passive targeting efficiency.[3-5] The size reduction design is mostly corresponding to the need in enhanced permeability and retention (EPR) effect of nanoparticles at the tumor sites compared with normal tissues, by which nano-carriers can pass through the relatively large gaps in blood vessels in tumor tissues, as compared to much compact normal blood vessels of just 2-6 nm in pore size.[6] Though the real particle size of MSNs has been successfully decreased to below 50 nm, these nanoparticles with such a small size always suffer from poor dispersity and instability in blood circulation owing to the large surface area and rich surface silanol groups. Polymer coating with single polyethylene glycol (PEG) or polyethyleneimine (PEI) has been reported previously to improve the dispersity of MSNs.[7,8] However, the single PEI modified MSNs could easily suffer from the fast blood clearance by the RES. Meanwhile, the dispersity of MSNs by single PEG coating is unsatisfactory as well, because the high ionic strength in the physiological media will compress the electric double layer on the particle surface, resulting in obvious decrease of the electrostatic repulsion between each nanoparticle. Compared to the above single polymer modification strategy, the combination of size

reduction, PEG coating and electrostatic repulsion in MSNs design, namely as "S-P-E" strategy, can significantly improve the EPR effect and passive targeting efficiency. In detail, the rapid movement of the flexible PEG chains can efficiently repel proteins from adsorption on particle surface, yielding stealth nanoparticles. Furthermore, the electrostatic repulsion can be realized by incorporation a high density of cationic group in the PEG framework, which can efficiently inhibit the compression of electric double layer in the high ionic medium, further improving the particle dispersity. Based on this combined strategy, Zink's group[9] recently reported the attachment of the PEI hyperbranched polymer with positive charge to cover the negatively charged surface of MSNs before PEG coating, showing the improved and high EPR effect of the modified MSNs compared with only PEG coating. However, this non-covalent interactions route induced poor chemical stability of surface polymer layer in the body circulation. Besides, in this system only 3.3 mg of doxorubicin (DOX) was loaded for every 100 mg MSNs, owing to the blocking of channel outlets by the adsorbed polymer. Therefore, for more rational design of MSNs drug carriers, the pore entrances should be open by the covalent modification of just accessible external surface using linear polymer chains with terminal reactive group, which will not block the pore entrances and therefore has little influence on drug loading amount. Therefore, aiming at future clinical application, a novel and efficient grafting method, integrating the "S-P-E" strategy, stable covalent polymer linking and high drug payload, is highly desired for the new generation of MSNs based DDSs.

Recent advances in organic active radicals and Reversible Addition Fragmentation chain Transfer (RAFT) polymerization allow for the synthesis of copolymer with tunable macromolecular architecture and chain length.[10,11] More importantly, by the RAFT polymerization route, a variety of acrylic monomers with distinctive performances, such as reaction-active, hydrophobic/hydrophilic, positive/negative-charged, temperature/pH value responsive and antifouling units, etc., can be controllably polymerized on the different solid surfaces, to synthesize a series of grafted polymers, such as well-defined homopolymers, diblock copolymers and random copolymers.[12-15] As far as we know, this is the first report on increasing EPR effect and drug therapeutic efficacy of MSNs-based DDSs, inspired by the design of polymer modification based on RAFT technique.

Meanwhile, two classic grafting methods, "Graft To" and "Graft From", can be performed *via* the RAFT polymerization strategy when the appropriate reactive groups are anchored onto the surface of solid support. The "Graft To" indicates that the end-functionalized polymer chains can be directly grafted onto the solid support, while the "Graft From" represents that the polymerization of monomers can proceed from the surface. Generally, the widely used "Graft To" approach always leads to a limited amount of grafted polymer owing to the steric barrier of earlier attached chains. Comparatively, the "Graft From" strategy is not limited by the steric effect and is therefore preferred in this study owing to its higher graft density, which is determined by density of the initiating groups on the particle surface.[16,17]

Herein, a combination strategy of "RAFT" and "Graft From" polymerization is proposed to decorate the surface of MSNs for the first time, which shows the great potential in improving the EPR effect of MSNs DDS. Such combined surface modification strategy has several distinctive advantages, including: 1) Efficient random copolymerization of two kinds of monomers, with PEG chain and quaternary amines, to enable the combined "S-P-E" strategy for the optimal EPR effect. 2) The spatial positive charging configuration, designed by incorporating the quaternary amines units into the PEG framework show the advantage of reduced toxicity due to the efficient screening of positive charge by PEG chains. 3) Higher grafting density of tethered polymer by "Graft From" approach compared to conventional "Graft To" route. 4) Higher DOX drug loading capacity owing to the open external outlets, compared to the previous PEI-PEG adsorption method. The *in vivo* experiments demonstrated that this modification strategy could bring both enhanced EPR effect of MSNs and prolonged blood circulation, which allow efficient DOX drug delivery to the Hela tumor-bearing in nude mice. This modification strategy is of great advantages for a range of nanomedicine applications, especially those based on DDS.

2. Experimental section

2.1 Synthetic process

2.1.1 Synthesis of MSN-NH_2

For preparation of MSNs, 4g cetyltrimethylammonium chloride (CTAC) and0.04 g triethanolamine (TEA) were dissolved in 40 mL of deionized water. Then, the mixed solution was heated to 95 ^{o}C in oil bath under intensive stirring. After 2 h, 6 mL of tetraethylorthosilicate (TEOS) was added dropwise under vigorous stirring. The reaction was processed for another 3h. The amine modified MSNs (MSN-NH_2) were synthesized by refluxing a certain proportion of aminopropyltriethoxysilane (APES) with MSNs in toluene overnight. To remove the CTAC surfactant in the pores of MSNs, the obtained particles were re-suspended in a solution of NaCl/methanol solution, and treated in an ultrasonic bath with temperature control at above 50 ^{o}C for 20 min every time followed by centrifugation. This procedure was repeated for three times, and the obtained MSN-NH_2 particles were dehydrated by heating the suspension up to 100 ^{o}C and sequentially collected by centrifugation for further use.

2.1.2 Synthesis of MSN-CTA

0.5 g 2-ethyl sulfonylthiocarbonyl 2-methyl propionic acid (CTA), 0.345 mL diisopropylcarbodiimide (DIC) and 0.388 mL diisopropylethylamine (DIPEA) were added into 5 mL CH_2Cl_2 in ice-water bath, and gently stirred for 30 min. Then 10 ml CH_2Cl_2 solution of MSN-NH_2 nanoparticles were dropwise added into 5 mL CH_2Cl_2 above. The reaction was performed for 48 hours at room temperature in the dark environment. At last, the particles were collected by centrifugation and washed by CH_2Cl_2, then stored at 4 ^{o}C for further use.

2.1.3 Synthesis of MSN-Poly(DMAEA-co-PEGMA)

RAFT polymerizations of PEGMA and DMAEA with a certain ratio were undertaken using 200 mg of MSN-CTA particles and using at 70 ^{o}C under argon atmosphere in presence of 1.0 mg of 2,2'-azobis(isobutyronitrile) (AIBN) as the initiators in 10 mL of dioxane solution. Typically for the ratio of 8:1, 0.083 mL of DMAEA solution, 1.93 mL of PEGMA and 15.0 mg CTA agents were sequentially added. The reaction flask was purged with argon for 30 minutes before heating up to 70 ^{o}C for 24 h.

2.1.4 Synthesis of MSN-PEG+

After purification procedure by centrifugation, MSN-Poly(DMAEA-co-PEGMA) was dispersed in dioxane solution. Then a trace amount of methyl iodide (MeI) were diluted by dioxane and dropwise added in the suspension, then mixed for 2 h in the dark environment under argon atmosphere. Finally, the particles were collected by centrifugation and repeated

washing by ethanol and water twice to remove the unreacted MeI.

2.2 Cell viability

PC-3, HK-2 and Hela were selected as cell models to evaluate the safety of MSN-PEG+. The cells were cultivated in Dulbecco's modified Eagle's medium (DMEM) containing 10%(v/v) fetal bovine serum, 100 units/mL penicillin and 100 mg/mL streptomycin in a humidified incubator at 37 ^{o}C, 5% CO_2.

In vitro cytotoxicities of MSN-PEG+ against cells were evaluated based on the 3-[4,5-dimethylthiazol-2-yl]-2,5-diphenyltetrazoliumbromide (MTT) assays. The cells were firstly seeded in 96-well plate at a density of 2×10^4 cells in 100 μL of DMEM solution overnight. The medium with different concentrations of MSN-PEG+ were added into the 96-well plate, and the cells were cultured for another 24 h. MTT with a concentration of 0.7 mg/mL in 100 μL of DMEM were added after removing the medium in wells. The cells proceed to be incubated in the incubator for 4 h. Then 100 μL of DMSO was added into each well after extraction of the original medium, and the absorption strength of every well at 490 nm was recorded by using a microplate reader (BioTek).

2.3 Measurement of DOX loading capacity

10 mg of MSN-PEG+ were suspended in 10 mL of PBS solution, then 5 mg of DOX drugwas added and stirred for 24h in the dark. The MSNs-PEG were collected by centrifugation and, then washed with PBS for three times. To measure the DOX payload of MSN-PEG+, the supernatant DOX solution was collected and its concentration was measured by the UV-visible absorption spectrum. The DOX loading capacity was measured by the below equation: Loading capacity (%) = 100 × (Total DOX -DOX in supernatant)/ (Total MSN-PEG used+ Total DOX -DOX in supernatant).

2.4 *In vivo* experiment details

Animal procedures were in agreement with the guidelines of the institutional Animal Care and Use Committee. Balb/c nude mice with weight about 22 g were obtained from the Laboratory Animal Center, Shanghai Tenth Hospital. In the blood chemistry evaluation, 6 nude mice were injected with 1 mg of MSN-PEG+ and DOX loaded MSN-PEG+, respectively. At 28 days after intravenous injection, the mice were sacrificed and the whole blood was collected for biochemical characterization. The blood parameters including WBC, RBC, HGB, HCT, MCV, MCH, MCHC, PDN, ALT, AST, BUN and Cr were measured by the JRDUN Biotechnology Co., LTD..

In the *in vivo* biodistribution experiment, Hela cells (0.2 mL, 5×10^6 cell/mL) were subcutaneously injected into nude mice, which began to be used after two weeks when the major diameter of the tumor reach about 1 cm. In the particle biodistribution experiment, 6 tumor-bearing nude mice were randomly divided to two groups (n=3), and intravenously injected by MSNs samples at the dose of 0.4 mg every mice, respectively. At 24 h after injection, the organs containing heart, liver, spleen, lung, kidney and tumor were collected and weighted for Si concentration measurement. To prepare the solution samples for ICP measurement, each organ received the treatment of digestion by concentrated $HClO_4/HNO_3$ (1:3) and sequent thermal-ablation by heating up to about 120 ^{o}C.

In the *in vivo* distribution experiment for VX_2 tumor-bearing New Zealand rabbits, 6 rabbits were randomly divided to 2 group (n=3). The sample at the dose of 15 mg was injected intravenously into the ear margin. At 24 h after injection, the Si concentration measurement was carried out as above in the nude mice experiment. To obtain the blood half-life of the MSN-PEG and MSN-PEG+, the blood of each rabbit were collected using the disposable hemostix in 2 min, 5 min, 10 min, 30 min, 1 h, 2 h and 24 h. 0.5 mL of blood sample were collected every time and the Si concentration were measured using ICP.

In the tumor inhibition experiment, 12 tumor-bearing nude mice were randomly divided to four groups (n=3), and received the intravenous injection of saline, empty MSN-PEG+, free DOX and DOX-loaded MSN-PEG+, respectively. The injection of samples was carried out in 0 and sixth day. The dosage of DOX-loaded MSN-PEG+ was 400 μg per animal, of which the corresponding DOX content was equal to the administration of free DOX (100 μg per mice). The weight and tumor volume were measured every three days for 12 days.

3 Results and discussion

3.1 Polymer chemistry coating

The overall synthetic process of surface modified MSNs is highlighted in Figure 1. Highly dispersed amine modified MSNs (MSN-NH_2) with uniform 50 nm size were fabricated following the previous reported route with a certain modification,[18] and the corresponding details of the synthesis are given in the Scheme S1. The BET surface area of MSN-NH_2 is 571 m^2/g measured by the N_2 sorption analysis as shown in Figure S1. The combined "RAFT" and "Graft From" polymerization was conducted in three stages. Firstly, the 2-ethyl sulfonylthiocarbonyl 2-methyl propionic acid was fabricated and employed as the chain transfer agent (CTA), of which the expected chemical structure was proved by ^{1}H-NMR (Figure S2).[19,20] The RAFT agent was successfully immobilized covalently onto MSN-NH_2 by amidation procedure using equal molar quantity of diisopropylcarbodiimide(DIC) and diisopropylethylamine(DIPEA) as catalysts. Secondly, the RAFT polymerization of PEGMA and PDMAEA with a certain ratio was carried out at 70 ^{o}C under argon atmosphere in presence of 2,2′-azobis(isobutyronitrile) (AIBN) as the initiators. Moreover, a certain amount of free RAFT agents were added into the reaction system, which could result in an accurate control of the polymerization and promote the growth of monomers on the particle surface. Thirdly, post-modification of surface copolymer (MSN-Poly(DMAEA-co-PEGMA) by using MeI enabled one-step conversion of tertiary amines to quaternary amine, and the final product, namely as MSN-PEG+, was thus obtained, as shown in the Figure 1. Herein, the quaternary amines were employed because of their stable structure and permanent positive charging in different pH environments, otherwise DMAEA monomers would gradually change into negatively charged carboxyl species after hydrolytic process. From Figures 2B,2C, the transmission electron microscopic (TEM) images show that the particle size of MSN-NH_2 and MSN-PEG+ are about 50 nm, and the scanning electron microscopic (SEM) image of MSN-PEG+ prepared *via* direct drying in the PBS solution (Figure 2D) proves high dispersity of the MSNs after the polymer surface modification.

Figure S3 shows the FTIR spectra of amine-modified MSNs (MSN-NH_2), chain transfer agent-modified MSN (MSN-CTA) and MSN-PEG+ nanoparticles. The band at 1737 cm^{-1} for ester group in MSN-PEG+ confirms the presence of the polymers. Meanwhile, the grafted copolymer on the MSNs surface was also confirmed by X-ray photoelectron spectroscopy (XPS) (Figure 2A). As revealed by the survey spectra, the significant increasing C1s/ Si2p ratio of MSN-PEG+ (33%/ 20%) compared with MSNs-CTA surface (16% / 28%), indicates the

successful coverage of MSNs with polymer. Moreover, the presence of N1s peak of MSN-CTA at 399.7eV is ascribed to the N-H species on the surface of particles. After RAFT polymerization, the N1s peak shifted to 402.6 eV corresponding to the quaternary amine species, demonstrating both successful grafting of the DMAEA on the MSNs and the sequent quaternization. The C1s spectrum of MSN-CTA exhibits two peak components at 284.9 and 288.5 eV, which are corresponding to the C–H and O=C–O groups of CTA. After reacting with monomers, the C1s peak at 286.7 eV appeared and became the strongest, which is in accordance with the C-O species of PEGMA units. Meanwhile, Figure S4 shows the zeta potentials are varied with pH values between 4 and 11 for the samples of MSN-CTA, MSN-Poly(DMAEA-co-PEGMA) and MSN-PEG+. The obviously increased surface potential (pH= 7.4) for the sample of MSN-PEG+ represents the increased positive charge density on their particles surface, further indicative of the successful modification with integrating the copolymer of positive charged quaternary amines and PEG coating. Besides, the weight proportion of the polymer brushes was measured to be ~8.0 % of the MSN-PEG+ by TG analysis (Figure S5).

Furthermore, the particles' positive zeta potential after quaternization was found at around 20.0 mV and presented weak changes when tuning the ratio of DMAEA/PEGMA from 1:8 to 1:2. It has been reported that larger proportion of quaternary amine group would induce higher exposure opportunity of positive charged units on the outermost layers, which could increase the particle toxicity.[21] Therefore, the optimal ratio DMAEA/PEGMA is 1:8 in this study, which can make the quaternary amine groups well-distributed and screened by the PEGMA units considering the random copolymeriztion route and different molecular lengths of two monomers. To further verify the bio-safety behavior of MSN-PEG+, a series of evaluations containing cell viability (Figure S6), and complete blood panel analysis for healthy bulb/c nude mice at a dosage of 10.5mg/kg MSN-PEG+ (Table S1) were carried out, and the results exhibited negligible toxicity and abnormity, compared with control group by only injection with PBS solution.

3.2 Comparison of particle dispersity and *in vivo* bio-distribution

Conventional nanoparticles used for passively targeting tumor sites by the EPR effect are always designed to possess minimum effective particle size and well dispersity in the physiological solution. PEG coating is one of the most extensively used strategies for the surface modification to realize good dispersity of nanoparticles.[22-26] In this study, MSNs with only PEG modification (MSN-PEG) has also been fabricated by the above combined "RAFT" and "Graft From" strategy, by just adding PEGMA monomers during the polymerization for comparison, as demonstrated in Figure S7. Figure 3A shows the results of dynamic light scattering analysis. When the MSNs modified only by PEGMA polymerization (MSN-PEG), more efficient improvement of particle dispersity with a mean size of 131.7 nm in PBS solution has been found. While, for the positively charged MSN-$N(CH_3)_3$+ modified by quaternary amine units (1-propanaminium,N,N,N-trimethyl-3-(trimethoxysilyl)-, chloride) just *via* an electrostatic repulsion route, obvious aggregation and precipitation can be visibly observed with greatly increased effective diameter (249.9 nm) in saline. It is worth noting that the hydrodynamic size of the synthesized MSN-PEG is much smaller than that in previous report by using conventional grafting strategy with linear PEG molecules,[25] which can be attributed to this "Graft From" strategy with high graft density. More significantly, MSN-PEG+ with enhanced positive-charging in the PEG external layers, shows an effective particle size of only 85.8 nm in PBS, very close to the size in pure water, such a size is considered to be approximately optimal to achieve a high EPR effect.[27] Meanwhile, the dispersion state and the long-term stability of MSNs-PEG+ can also be evaluated quantitatively by UV–vis spectroscopy (Figure S8). According to this figure, no clear reduction in UV-vis absorption strength at wavelength of 289 nm can be found from the suspension of MSN-PEG+ both in pure water and PBS, showing the excellent stability of MSNs-PEG+ for at least three days. It is very interesting that the combination of PEG layer for steric hindrance with high zeta potential value yield significantly different dispersity behavior.

In order to determine whether the design of MSN-PEG+ can improve the tumor accumulation of MSNs compared to MSN-PEG without cationic modification, Si quantification analysis using inductively coupled plasma mass spectrometry(ICP) was performed in the nude mice model xenografted with Hela cells. Two kinds of nanoparticles with the same amount of 400 μg were intravenously injected into the nude mice, and all the major organs (liver, spleen, lung, heart, kidney and tumor) were collected to examine the Si concentrations. Very interestingly, clear differences can be found in the level of liver accumulation between two MSNs with different surface chemistry modifications. As shown in Figure 3B, compared to MSN-PEG, MSN-PEG+ shows a distinctive reduction in reticuloendothelial system (RES) uptake in 24 hours (23.25% for MSN-PEG vs 9.15% for MSN-PEG+), and substantially increased accumulation at tumor site (6.7% for MSN-PEG+, vs 2.9% for MSN-PEG).The significantly enhanced tumor accumulation of MSNs-PEG+ could be attributed to the use of PEG+ coating, resulting in the smallest possible hydrodynamic size and the optimal condition of dispersity, providing much more possibility for MSNs to pass through the gaps in tumor vessels, as shown in the schematic Figure 3C.

Furthermore, the *in vivo* distributions and blood half-life at 24 h post-injection with each sample into VX_2 tumor-bearing New Zealand rabbits were also conducted for comparison. The quantitative results of ICP (Figure 4) also confirm the similar reduction in RES uptake for MSN-PEG+, i.e., much less MSN-PEG+ nanoparticles were cleared through liver and spleen. Moreover, the estimated ICP data demonstrated significantly higher particle concentration of MSN-PEG+ (8.4 μg/g) at tumor site than that of MSN-PEG (4.7 μg/g). Meanwhile, the collected blood samples of 500 μL in different time intervals were eluted and used for quantitative analysis of the Si concentrations. These blood half-life results show remarkably delayed blood clearance for MSN-PEG+ (~112 min), compared with those of MSN-PEG (~53 min), and MSN-$N(CH_3)_3$+ (~7 min). The shortest time duration of MSN-$N(CH_3)_3$+ with positively charged surface in blood stream may be due to the dramatic immune response triggered by its nonspecific binding to serum proteins. In contrast, although MSN-PEG+ is also positively charged, the positive charge on a moderate amount of quaternary ammonium units can be mostly screened by spatial PEG chains, which is favorable for suppressing the particle opsonization and capture by the RES. In a word, the MSN-PEG+ nanoparticles exhibit similar and distinctly enhanced EPR effect in both nude mice and rabbit tumors models.

3.3 DOX delivery by MSN-PEG+ nanoparticles

DOX is an effective and commonly used drug for treatment of malignant tumors, however, the short half-life time and

severe side effect of its free drug formulation limit its widespread use in clinic therapy.[28] To confirm the improved treatment efficacy by MSN-PEG+ DDS, four groups of nude mice with established xenografts of Hela cells received the administration of (1) saline, (2) empty MSN-PEG+ without drug loading, (3) free DOX and (4) DOX loaded MSN-PEG+, for comparison. As we known, MSNs with negative silanol surface perform strong electrostatic interaction with positively charged DOX, leading to a large amount and high efficiency of DOX loading.[29] In the MSN-PEG+, though positively charged on outer surface, the synthetic strategy ensures the free diffusion of DOX into mesopore structure *via* the open pore entrance, thus the payload of as high as 25% of total DDS and the loading efficiency of 66 % can be achieved (Figure S9). Meanwhile, no significant changes of zeta-potential was found in MSN-PEG+ after DOX loading (21.1 mV), compared to no-loaded MSN-PEG+ (20.0 mV), which demonstrated the positive surface charge of MSN-PEG+ could efficiently decrease the adsorption of free DOX drug on the particle surface. More importantly, in this MSN-PEG+ delivery system, no obvious drug release was found in the physiological solution with pH 7.4 as shown in Figure S10, demonstrating the negligible drug release in the blood circulation. However, the DOX loaded MSN-PEG+ showed a rapid drug release when being soaked in the acid solution (pH 5.5). It is considered that this pH-responsive drug release could efficiently decrease the side-effect of chemotherapy and further increase the drug effect on the tumor. The intravenous injections were carried out when the average diameter of tumor reached 1 cm (about 2 weeks after inoculation). The dosage of DOX in the drug administration was 100 μg per animal and all injections were performed every six days until the end of the experiment (12 days). On the 12th day of post-administration, comparable growth rates (Figure 5A, 5B) were evaluated in each group with the relative tumor volumes (V/Vo) being measured to be 4.66±1.44 (group 1), 4.37±0.31 (group 2), 2.68±0.85 (group 3) and 1.46 ± 0.39 (group 4), respectively. It is clear that no obvious tumor inhibitions can be found in the nude mice with both saline control and empty MSN-PEG+ nanoparticles, while the data shows a 68.7% inhibition rate for DOX loaded MSN-PEG+ compared to 42.5% for the free DOX ($P \leq 0.005$). More importantly, consistent with the tumor inhibition results, a significant increase in DNA strand breaks has been found compared with free DOX formulation, being represented by the green fluorescence dots from TUNEL staining assay (Figure 5C) at tumor sites. The significant enhancement in the inhibition rate for DOX loaded MSN-PEG+ nanocarriers can be ascribed to both the longer retention time of drug in the blood circulation and the enhanced EPR effect.

Body weight changes in tumor-bearing nude mice were measured every three days. Nevertheless, no profound weight decreases were found in group 3 and 4 during the process (Figure 6A)，probably owing to the low dosage of DOX used in our experiment. Meanwhile, the blood chemistry and complete blood panel profiles (Table S2) show the biosafety of DOX drug delivery using the MSNs-PEG+ nanocarriers. In contrast, the side effect of free DOX was observed in heart section by hematoxylin and eosin (H&E) staining, as shown in Figure 6B, the administration of free DOX has led to noticeable cardiac muscle fiber degeneration. In contrast, there is no distinct acute cardiac toxicity by both empty carrier and DOX loaded MSN-PEG drug carrier. The reduction of cardiotoxicity should be due to the change of pharmacokinetic behavior of DOX inside the carrier, also the very slight loss of DOX from MSN-PEG+ during blood circulation.[30] In addition, no noticeable tissue damages and adverse effects of both free DOX and DOX loaded MSN-PEG+ samples to other organs, such as kidney, liver, spleen and lung, as shown from Figure 7 can be found.

Meanwhile, the urine and feces of New Zealand rabbits were collected before and after the injections of MSN-PEG+ samples at different time points in 2 h, 24 h, 48 h and 72 h. As shown in Figure S11, in the first 24 h after injection, the cumulative release amount from urine and feces is approximately 8 % and 52 %, respectively. Meanwhile, it can be found that a majority of Si elements (about 98% of total Si injected) can be excreted out of body through urine and feces within 72 h. The above evidences confirmed the satisfactory biosafety of MSNs-PEG+ as anticancer drug carrier, which is consistent with the results of complete blood panel files and biochemistry results.

4 Conclusions

In summary, a novel surface modification route by copolymer of quaternary amines and PEGMA units using a combined "RAFT" polymerization and "Graft From" strategy, is proposed on 50 nm-sized MSNs. We found that this surface modification strategy could significantly increase the EPR effect and tumor accumulation of MSNs in the tumor site, leading to higher tumor growth inhibition effect than free drug by the in *vivo* study. More importantly, this novel MSN-PEG+ DDS can greatly reduce the side effect of DOX administration and offer high biosafety. Thus, based on the combination polymerization strategy, it is expected that a series of acrylic monomers with reactive groups, especially the N-acryloxysuccinimide, can also be introduced to the PEG framework towards the efficient covalent binding with other functional molecules, such as tracking probes and targeting biomolecules, to realize the multifunctional applications in addition to drug delivery.

Acknowledgements

We greatly acknowledge financial support from the National Basic Research Program of China (973 Program, Grant No.2011CB707905), China National Funds for Distinguished Young Scientists (51225202), National Natural Science Foundation of China (Grant No. 51072212, 51132009, 81371570), and Program of Shanghai Subject Chief Scientist (Grant No.14XD1403800).

Notes and references

[a]State Key Laboratory of High Performance Ceramic and Superfine Microstructures, Shanghai Institute of Ceramics, Chinese Academy of Science, Shanghai, 200050 , (P.R.China)

[b]Tenth Peoples Hospital of Tongji University, Shanghai, 200072, (P. R. China)

Electronic Supplementary Information (ESI) available: Experimental details and characterization data. See DOI: 10.1039/b000000x/

1 Wu, S. H.; Mou, C. Y.; Lin, H. P. Chem. Soc. Rev. 2013, 42, 3862.

2 Ehlert, N.; Mueller, P. P.; Stieve, M.; Lenarz, T.; Behrens, P. *Chem. Soc. Rev*. 2013, **42**, 3847.

3 Ma, K.; Werner-Zwanziger, U.; Zwanziger, J.; Wiesner, U. *Chem. Mater*. 2013, **25**, 677.

4 Lu, J.; Liong, M.; Li, Z. X.; Zink, J. I.; Tamanoi, F. *Small* 2010, **6**, 1794.
5 Tarn, D.; Ashley, C. E.; Xue, M.; Carnes, E. C.; Zink, J. I.; Brinker, C. *J. Accounts. Chem. Res.* 2013, **46**, 792.
6 Iyer, A. K.; Khaled, G.; Fang, J.; Maeda, H. *Drug Discov. Today* 2006, **11**, 812.
7 Zhu, Y. F.; Ikoma, T.; Hanagata, N.; Kaskel, S. *Small* 2010, **6**, 471.
8 Rosenholm, J. M.; Meinander, A.; Peuhu, E.; Niemi, R.; Eriksson, J. E.;Sahlgren, C.; Linden, M. *Acs Nano* 2009, **3**, 197.
9 Meng, H.; Xue, M.; Xia, T.; Ji, Z. X.; Tarn, D. Y.; Zink, J. I.; Nel, A. E. *Acs Nano* 2011, **5**, 4131.
10 McLeary, J. B.; Klumperman, B. *Soft Matter* 2006, **2**, 45.
11 Moad, G.; Rizzardo, E.; Thang, S. H. *Aust. J. Chem.* 2005, **58**, 379.
12 Perrier, S.; Takolpuckdee, P.; Mars, C. A. *Macromolecules.* 2005, **38**, 6770.
13 Roy, D.; Guthrie, J. T.; Perrier, S. *Macromolecules*. 2005, **38**, 10363.
14 Rowe, M. D.; Thamm, D. H.; Kraft, S. L.; Boyes, S. G. *Biomacromolecules* 2009, **10**, 983.
15 Sun, J. T.; Yu, Z. Q.; Hong, C. Y.; Pan, C. Y. *Macromol. Rapid. Comm.* 2012, **33**, 811.
16 Li, C. Z.; Benicewicz, B. C. *Macromolecules.* 2005, **38**, 5929.
17 Li, Y.; Benicewicz, B. C. *Macromolecules.* 2008, **41**, 7986.
18 Kobler, J.; Moller, K.; Bein, T. *Acs Nano* 2008, **2**, 791.
19 Lai, J. T.; Filla, D.; Shea, R. *Macromolecules.* 2002, **35**, 6754.
20 Convertine, A. J.; Lokitz, B. S.; Vasileva, Y.; Myrick, L. J.; Scales, C. W.; Lowe, A. B.; McCormick, C. L. *Macromolecules.* 2006, **39**, 1724.
21 Sun, J. T.; Hong, C. Y.; Pan, C. Y. *Journal of Physical Chemistry C* 2010, **114**, 12481.
22 Sperling, R. A.; Parak, W. J. *Therapeutic Innovation & Regulatory Science* 2013, **47**, 1333.
23 Cauda, V.; Argyo, C.; Bein, T. *J. Mater. Chem.* 2010, **20**, 8693.
24 Hamidi, M.; Azadi, A.; Rafiei, P. *Drug Deliv.* 2006, **13**, 399.
25 He, Q. J.; Zhang, J. M.; Shi, J. L.; Zhu, Z. Y.; Zhang, L. X.; Bu, W. B.; Guo, L. M.; Chen, Y. *Biomaterials.* 2010, **31**, 1085.
26 He, Q. J.; Zhang, Z. W.; Gao, F.; Li, Y. P.; Shi, J. L. *Small* 2011, **7**, 271.
27 Ruoslahti, E.; Bhatia, S. N.; Sailor, M. J. *J. Cell Biol.* 2010, **188**, 759.
28 Xiong, X. B.; Ma, Z. S.; Lai, R.; Lavasanifar, A. *Biomaterials.* 2011, **32**, 4194.
29 Ma, M.; Chen, H. R.; Chen, Y.; Wang, X.; Chen, F.; Cui, X. Z.; Shi, J. L. *Biomaterials.* 2012, **33**, 989.
30 Du, X. H.; Jin, R. S.; Ning, N.; Li, L.; Wang, Q. S.; Liang, W. T.; Liu, J. C.; Xu, Y. X. *Oncol. Rep.* 2012, **28**, 1743.

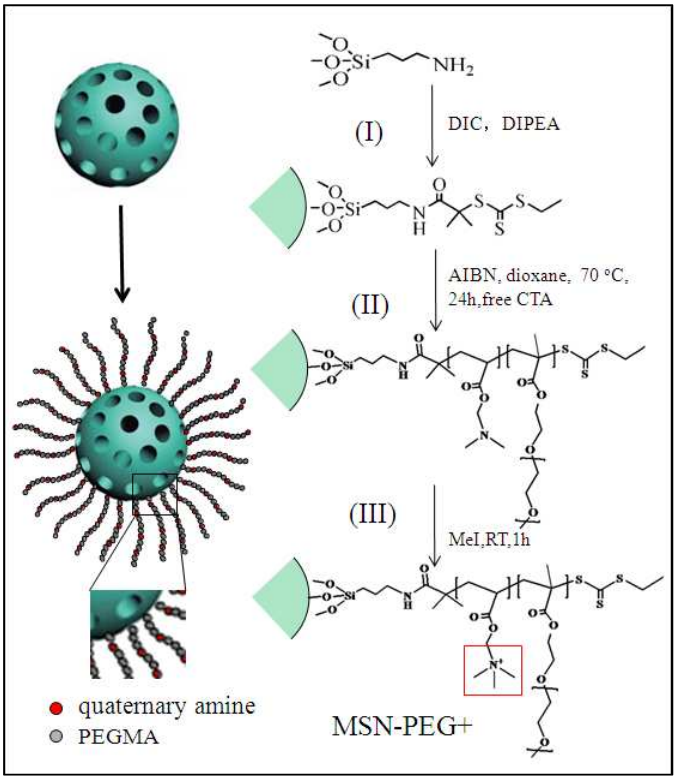

Figure 1. Synthetic scheme of MSN-PEG+ with positively charged PEG external layer, the random copolymer backbones of two monomers were synthesized by the RAFT mediated polymerization.

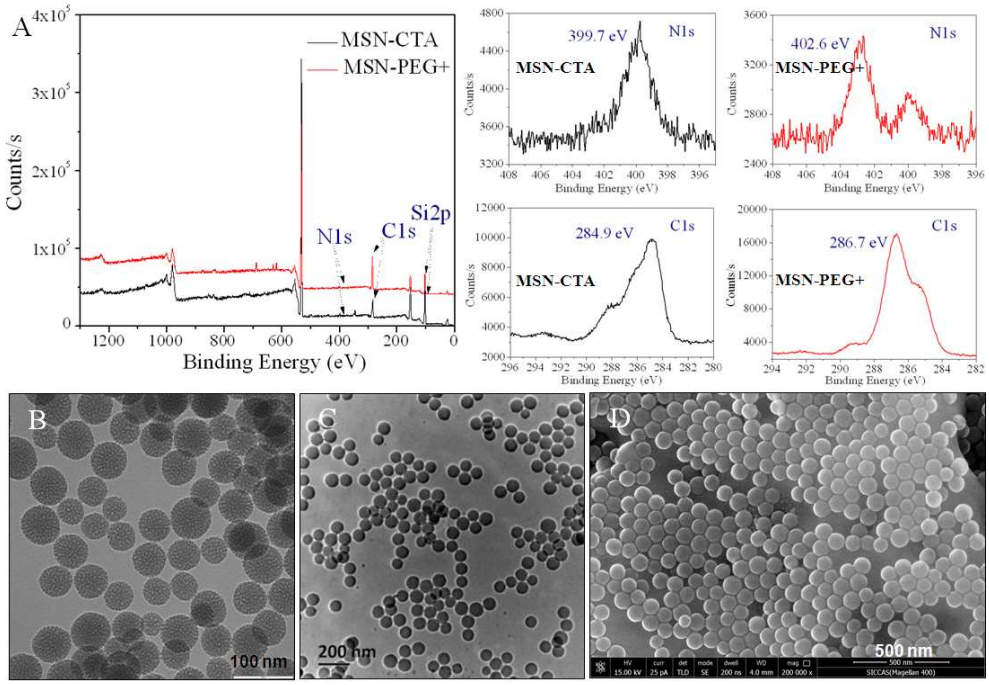

Figure 2. (A) Survey spectra of MSN-CTA and MSN-PEG+, and their corresponding XPS N1s and C1s peaks. (B, C) TEM images of (B) MSN-NH_2 and (C) MSN-PEG+. (D) SEM image showing high dispersity of MSN-PEG+ prepared *via* direct drying in the PBS solution.

A

Particle Type	Mean Size (TEM)	Mean Size in H_2O	PDI in H_2O	Mean Size in PBS	PDI in PBS	Zeta Potential in H_2O
MSN-PEG	50 nm	79.2 nm	0.104	131.7 nm	0.152	-10.9 mV
MSN-PEG+	50 nm	85.3 nm	0.104	85.8 nm	0.122	+20.0 mV
MSN-$N(CH_3)_3$+	50 nm	134.8 nm	0.192	249.9 nm	0.361	+22.7 mV

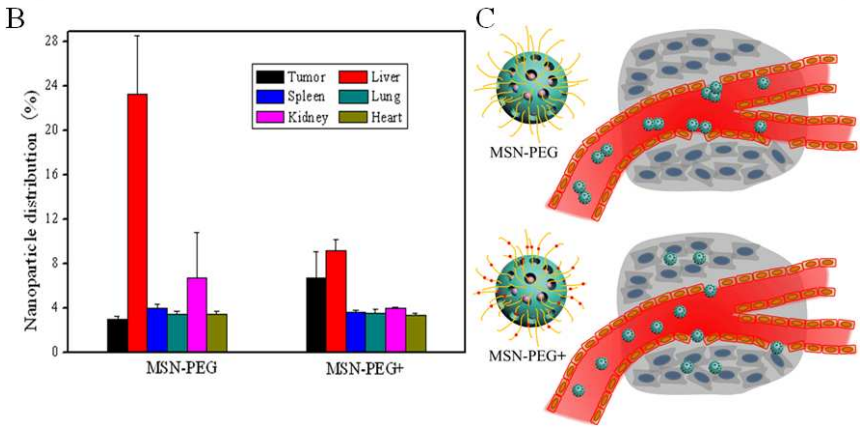

Figure 3. (A) Particle sizes and zeta potentials of MSN-PEG, MSN-PEG+ and MSN-$N(CH_3)_3$+ in pure water and PBS solution. (B) *In vivo* distribution of Si element in tumor-bearing nude mice in 24 h post-injection of MSN-PEG and MSN-PEG+. The percentages were calculated by the formula (Si weight in each tissue/the total Si weigh of injected particles. Obviously higher Si concentration was found in MSN-PEG+, compared to that of MSN-PEG ($P \leq 0.005$). (C) The schematic diagram showing that the EPR effect could be enhanced by decreasing the particle size and improving the dispersity.

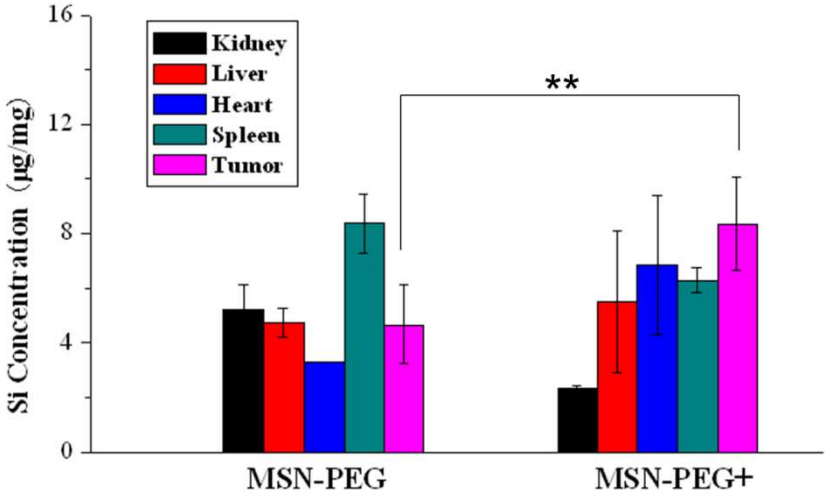

Figure 4. *In vivo* distribution of Si element concentration in VX_2 tumor-bearing rabbit at 24 h after injection of MSN-PEG and MSN-PEG+. ** denoted in the figure represents significant difference in Si concentration distribution by comparing the MSN-PEG with MSN-PEG+ group at $P \leq 0.005$.

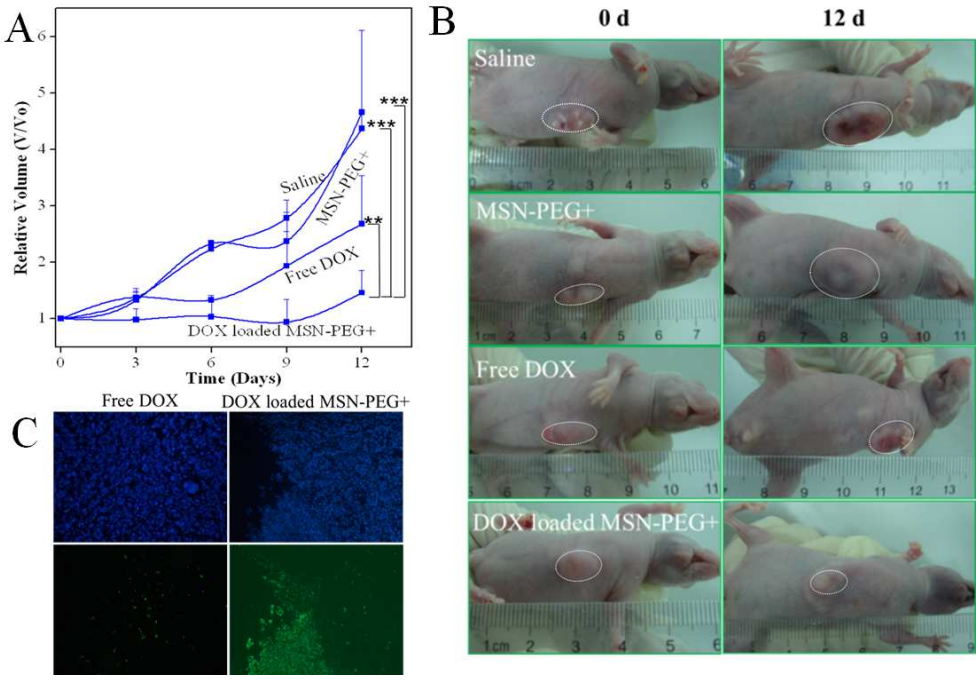

Figure 5. *In vivo* tumor growth inhibitions of tumor–bearing nude mice after intravenous injection of DOX-loaded MSN-PEG+. (A) Time dependent tumor growth curves in 3 d, 6 d, 9 d and 12 d after the injections of saline, empty MSN-PEG+, free DOX and DOX loaded MSN-PEG+. The dosage of DOX drug was 100 μg per mice for each administration every six days. ** and *** represents significant difference in tumor growth inhibition found by comparing the four groups at $P \leq 0.005$ and $P \leq 0.0005$, respectively. (B) The photographs of nude mice before and at the end of treatment showing the different tumor growth inhibition effects. (C) The TUNEL staining assay showing enhanced apoptosis and cell death by DOX loaded MSN-PEG+ compared to free DOX. The above blue fluorescence images are the cell nucleus after DAPT staining. The green fluorescence in the below images (200×) represent of the TUNEL positive cells.

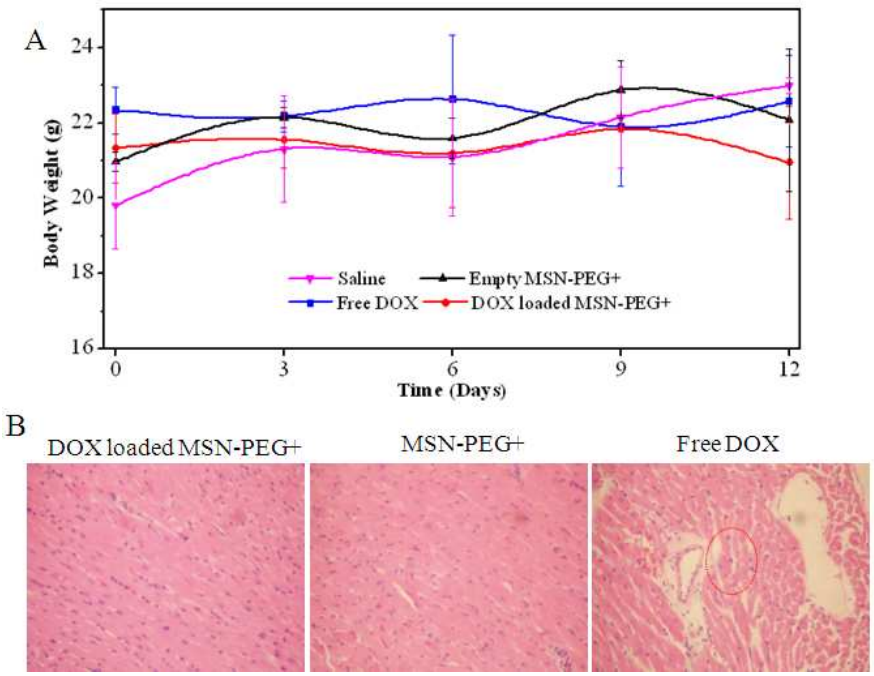

Figure 6. (A) Mice weight recorded every three days. (B) Histological analysis of heart after treatment of DOX loaded MSN-PEG+, empty MSN-PEG+ and free DOX. The tissue section were stained by H&E and sequentially detected by microscopy (200×).

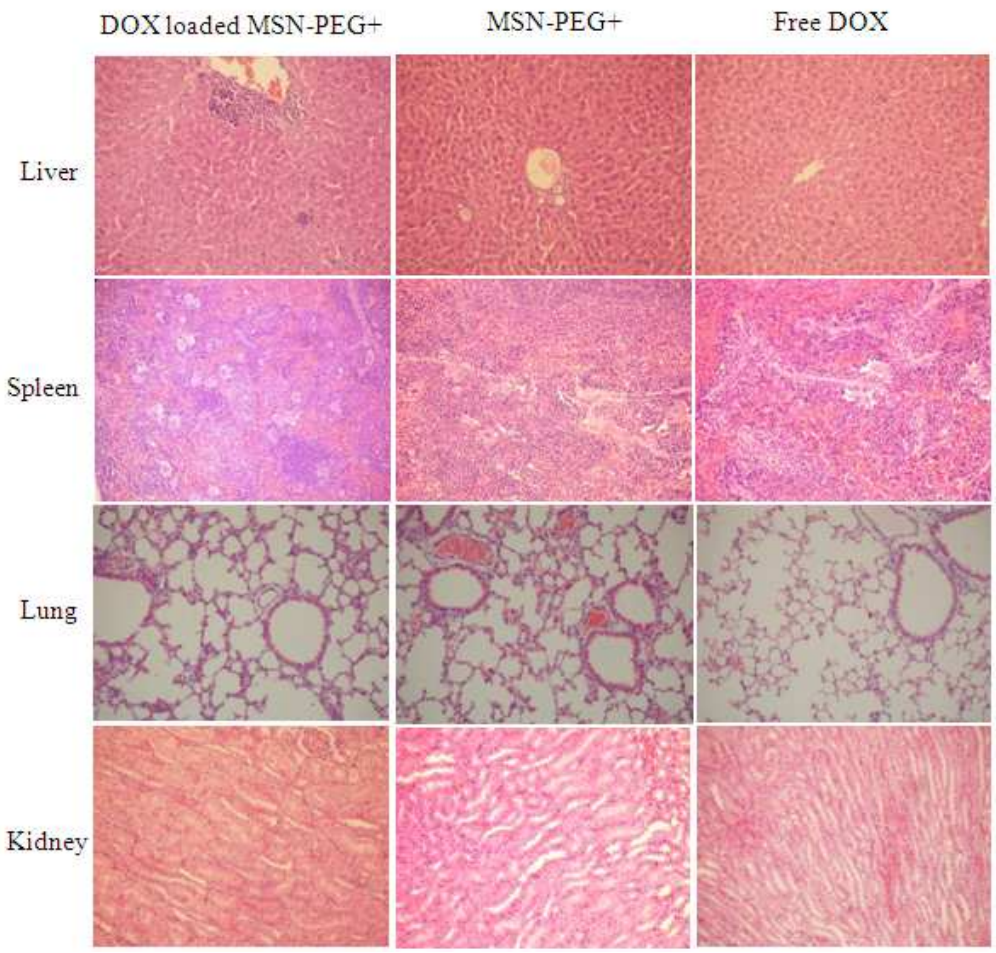

Figure 7. H&E stained tissue section from tumor-bearing nude mice at 24 h after injection of DOX-loaded MSN-PEG+, empty MSN-PEG+, and free DOX, respectively. No obvious tissue damage and adverse effect were shown from the liver, spleen, lung and kidney of these groups.

TOC